Vol. 394: 35–48, 2009
doi: 10.3354/meps08270

MARINE ECOLOGY PROGRESS SERIES
Mar Ecol Prog Ser

Published November 18

OPEN ACCESS

Carbon and nitrogen cycling on intertidal mudflats of a temperate Australian estuary. IV. Inverse model analysis and synthesis

Perran L. M. Cook[1,*], Dick Van Oevelen[2], Karline Soetaert[2], Jack J. Middelburg[2,3]

[1]Water Studies Centre, Monash University, Clayton 3800, Victoria, Australia
[2]Centre for Estuarine and Marine Ecology, Netherlands Institute of Ecology, Korringaweg 7, 4401 NT Yerseke, The Netherlands
[3]Faculty of Geosciences, Utrecht University, PO Box 80021, 3508 TA Utrecht, The Netherlands

ABSTRACT: Microphytobenthos (MPB) are recognised as exerting an important controlling influence over C and N flows in euphotic sediments; however, the coupling between these flows remains poorly studied. We undertook an inverse model analysis of C and N fluxes through the microbial compartment on intertidal flats in a temperate estuary. The analysis showed that the trophic balance of the sediment exerted a strong influence on the relative fluxes of C and N through the sediment microbial community. Under increasingly autotrophic conditions (production:respiration >1), the assimilation of C relative to N rose above the cellular C:N ratio of MPB, resulting in increased excretion rates of organic matter by MPB. The C:N ratio of the organic matter excreted was also highly variable, ranging from ~20 (mol:mol) under heterotrophic conditions, and increasing to >50 under autotrophic conditions. The relative fluxes of C and N through bacteria were also significantly affected by the trophic balance of the sediment and the ratio of C:N mineralized by bacteria was significantly higher under autotrophic conditions. Dissolved organic N release by bacteria and uptake by MPB also predominated over inorganic N forms under autotrophic conditions. We conclude that C and N fluxes through shallow euphotic sediments may become significantly decoupled and well above the commonly assumed Redfield ratio and measured cellular C:N ratios of MPB.

KEY WORDS: Nitrogen · Carbon · Sediment · Microphytobenthos · Stoichiometry · Inverse model

INTRODUCTION

Tidal flats have been found to perform a number of important ecological functions including providing a source of organic C to consumers (Kang et al. 2003) as well as being both an important source and sink for nutrients (Joye et al. 2009). Microphytobenthos (MPB) are increasingly recognised as playing a pivotal role as a C source to heterotrophic consumers, as well as modulating the flux of nutrients across the sediment water interface (e.g. Sundbäck et al. 1991, Middelburg et al. 2000). MPB are known to direct a large fraction of photosynthesis into the excretion of a wide range of organic compounds (referred to here as extracellular organic material, EOM). It has been observed that EOM production increases significantly as a consequence of nutrient limitation (Staats et al. 2000, Underwood & Paterson 2003). The production of EOM has a number of important implications for the fluxes of C and nutrients (in particular N) through the microbial community. EOM can act as an important source of C for bacteria (Middelburg et al. 2000, Goto et al. 2001, Cook et al. 2007); however, it is relatively N poor, consisting predominantly of carbohydrates (Staats et al. 1999, Granum et al. 2002). As a consequence, it is likely that bacteria assimilating EOM will immobilize

*Email: perran.cook@sci.monash.edu.au

N and P into their biomass (Goldman et al. 1987, Sterner & Elser 2002). Consistent with this, studies using $^{15}N\text{-}NH_4^+$ have shown that bacteria strongly retain N within estuarine sediments (Blackburn & Henriksen 1983, Veuger et al. 2007, Gribsholt et al. 2009). It has also been shown that MPB may have a strong negative influence on nitrification within sediments and it was hypothesized that this arose as a consequence of NH_4^+ assimilation by bacteria consuming exudates from MPB (Risgaard-Petersen 2003, Risgaard-Petersen et al. 2004). High rates of EOM production are also consistent with a low release of dissolved inorganic N (DIN) relative to dissolved inorganic C (DIC) in shallow euphotic environments (Lomstein et al. 1998, Cook et al. 2004a,b, Ferguson et al. 2004b, Eyre & Ferguson 2005).

Because nutrient status plays a critical role in the rates of EOM production, the importance of EOM is likely to vary strongly as a function of nutrient demand versus nutrient availability (Underwood 2002). Previous studies have shown that the production to respiration (P:*R*) ratio of the sediment is a useful metric of MPB activity and has a strong influence on the nutrient demand of the sediments (Rizzo et al. 1996, Ferguson et al. 2004b, Engelsen et al. 2008). At P:*R* > 1, sediments tend to be a sink for nutrients as a consequence of MPB nutrient requirements exceeding the capacity of the sediments to supply nutrients, making MPB most likely nutrient-limited under these conditions. At P:*R* < 1, sediments will be a source for nutrients, with the capacity of the sediments to supply nutrients exceeding the assimilative requirements of MPB, so that MPB are highly unlikely to become nutrient-limited. Furthermore, the sediment P:*R* ratio has also been shown to have a strong influence over benthic denitrification rates and the relative importance of organic nutrient fluxes, highlighting its strong influence over a range of microbial processes (Risgaard-Petersen 2003, Ferguson et al. 2004b, Engelsen et al. 2008).

To date, there have been no attempts to create a coherent mass balanced model describing the fluxes of C and N within the microbial community of euphotic shallow water sediments. This is essential in order to better understand the role of EOM in mediating the relative fluxes of C and N through microbial communities and how this varies with potentially important drivers such as sediment P:*R* ratio. The construction of such models is generally limited by the fact that it is logistically and technically impossible to measure all of the fluxes occurring within the system. Inverse analysis techniques have been developed to reconstruct such mass balances from scattered and incomplete data sets (Vézina & Platt 1988). Inverse analysis techniques merge a preconceived model structure with measured and literature data on pool sizes, physiological rates and fluxes between pools to create a coherent mass-balanced picture of the system in question. Furthermore, data sets which undergo inverse analysis are checked for internal consistency and can be analyzed for residual uncertainty (Van Oevelen et al. 2006a). Soetaert & Van Oevelen (2009) provide a practical guide on inverse modeling in food webs research with pedagogical examples.

Here we applied inverse analysis to a previously published data set collected from intertidal flats in a mesotrophic estuary which covers a wide range of seasons, metabolic conditions and ranges from sediments that are heterotrophic to highly autotrophic (Cook et al. 2004a,b,c). Of key interest here were the flows of C and N between algae and bacteria which were reconstructed by the model. We hypothesised that the most autotrophic sediments would be nutrient limited, have high rates of EOM production and result in a departure of the C:N flux ratio away from the cellular C:N ratio. By contrast, heterotrophic sediments would be nutrient replete, resulting in lower C excretion rates, and a closer coupling between C and N flows at near cellular stoichiometry.

MATERIALS AND METHODS

Site description. The inverse model analyses were performed on data collected over 4 seasons from the upper and lower regions (~0.5 m elevation difference) of 2 mudflats in the Huon Estuary in Southeast Tasmania, Australia (Fig. 1). The mudflats chosen for this study were located at Port Cygnet (Site PC) and Castle

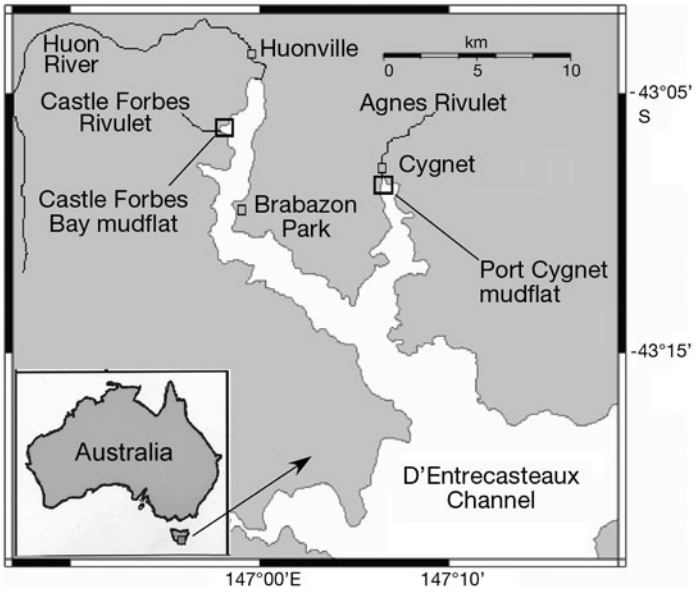

Fig. 1. Huon Estuary, Southeast Tasmania, Australia. Location of study sites at Castle Forbes Bay (CF) and Port Cygnet (PC)

Forbes Bay (Site CF), which are separated by a distance of 9 km. Site PC is a somewhat isolated, marine dominated side-arm of the estuary, with small and sporadic discharge from 2 rivulets. Site CF was located in the upper estuary, which is heavily influenced by discharge from the Huon River, resulting in the waters at this site having a lower salinity than at Site PC. More detailed site descriptions are given by Cook et al. (2004a). Nutrient concentrations within the Huon Estuary are generally low (total N < 20 µM, NOx < 7 µM, total P < 1 µM, and filterable reactive P < 0.5 µM) and the estuary is classed as mesotrophic (Butler et al. 2000).

Inverse method. Detailed studies of the biology and biogeochemistry of these study sites have previously been published and included measurements of benthic metabolism, benthic N fluxes, sediment N mineralisation rates, N and organic matter pool sizes as well as algal and microbial biomass (Table 1). We merged these data in an inverse model to obtain a consistent mass-balanced picture of the C and N cycling in these temperate sediments. The focus was on the microbial pools (algae and bacteria) and their uptake and excretion of organic and inorganic nutrients and C. We did not consider other biota, such as meio- or macrobenthos beyond a grazing term. We justify this on the basis that the bulk of the C and N fluxes will be through the algal and bacterial pools (e.g. Van Oevelen et al. 2006a, Veuger et al. 2007), and that the abundance of benthic infauna was found to be low (Cook unpubl. data), although we have no information on meiofauna, which may or may not be an important grazing component (Middelburg et al. 2000, Pinckney et al. 2003, Van Oevelen et al. 2006a)

The inverse model structure considers fluxes of C and N among the biotic pools' MPB, heterotrophic bacteria (BAC), grazers (GRAs), and the abiotic pools' dissolved organic matter (DOM) and particulate organic

Table 1. Stocks and flux data used in the inverse analysis. MPB = microphytobenthos, DOC, DON = dissolved organic carbon and nitrogen, respectively; POC, PON = particulate organic carbon and nitrogen, respectively; DIC = dissolved inorganic carbon

Parameter	Description	Unit	Source
MPB carbon	Calculated from chl *a* data using a measured C:chl *a* of 20	mmol C m^{-2}	Cook et al. (2004a)
MPB C:N	Range and average value from the 2 sites over summer months. Model run with values of 5, 8, 15	mol C mol N^{-1}	Cook et al. (2004c)
MPB nitrogen	Calculated from MPB C and C:N (see above)	mmol N m^{-2}	
DON nitrogen	Autumn and summer values	mmol N m^{-2}	P. Cook unpubl. data
DOC carbon	Based on DOM C:N ratio (see literature data)	mmol C m^{-2}	Burdige & Zheng (1998)
Bacterial carbon	Based on fatty acid data of the top 0.5 cm that are extrapolated to the top 8 cm of sediment by fitting with an exponential function	mmol C m^{-2}	Cook et al. (2004c); P. Cook (unpubl. data)
Bacterial C:N	Assumed to be 5	mol C mol N^{-1}	Goldman & Dennett (2000)
Bacterial N	Calculated from bacterial C and C:N (see above)	mmol N m^{-2}	
NH_4^+ pool	NH_4^+ concentrations in the porewater integrated over 8 cm	mmol N m^{-2}	Cook et al. (2004b)
POC	Particulate organic C over the top 8 cm of sediment	mmol C m^{-2}	Cook et al. (2004c)
PON	Particulate organic N over the top 8 cm of sediment	mmol N m^{-2}	Cook et al. (2004c)
Total sediment respiration	DIC fluxes in retrieved cores	mmol C m^{-2} d^{-1}	Cook et al. (2004a)
Net ammonia production in sediment	From porewater ammonia profiles, assuming steady-state	mmol N m^{-2} d^{-1}	Cook et al. (2004b)
Net DON flux	DON fluxes measured in retrieved cores	mmol N m^{-2} d^{-1}	Cook et al. (2004b)
Benthic primary production	Calculated as net light DIC assimilation – dark DIC production scaled to day length	mmol C m^{-2} d^{-1}	Cook et al. (2004a)
Nitrogen fixation	Measured (offset by one year relative to all other measurements) in retrieved cores using the acetylene reduction assay calibrated with ^{15}N	mmol N m^{-2} d^{-1}	Cook et al. (2004b)
NH_4^+ assimilation from sediment	Net NH_4^+ production in the sediment minus sediment efflux of NH_4^+ measured in core incubations	mmol N m^{-2} d^{-1}	Cook et al. (2004b)
NH_4^+ assimilation from water column	Net NH_4^+ influx to the sediment measured in core incubations	mmol N m^{-2} d^{-1}	Cook et al. (2004b)
NO_3^- assimilation from water column	Net NO_3^- influx into the sediment minus denitrification	mmol N m^{-2} d^{-1}	Cook et al. (2004b)

matter (POM), their C stock and C:N ratio (Fig. 2 and Table 2). The MPB pool comprises both eukaryotic and prokaryotic primary producers (algae and cyanobacteria). MPB fix inorganic C (DIC) and N (as N_2) and take up nitrate (NO_3), ammonium (NH_4^+) and organic N (DON) from the water column (w) and/or sediment. We assume that all N uptake can either lead to the production of MPB biomass or is excreted as EOM and the C:N ratio of MPB couples the N production to biomass production of C. Carbon fixation in excess of the C required for biomass production is excreted as EOM. Based on 4 measurements made during summer, the C:N ratio of MPB was found to vary between 5 and 15 (mol:mol) among sites and seasons. As the C:N ratio was not always quantified, the model was run 3 times for each site and season with cellular MPB C:N ratios fixed at 5, 8 and 15 to check for the sensitivity of the results to this value. BAC take up C and N from DOC and DON, but produce biomass in a fixed C:N ratio: excess C or N is excreted as DOM. POM deposition from the water column fuels the POM in the sediment and is hydrolysed by bacteria to DOM. Grazing by benthic fauna of MPB and BAC is considered a loss process of C and N from the system. Another loss process of C for MPB and BAC is respiration. In addition, BAC respire N in the form of NH_4^+.

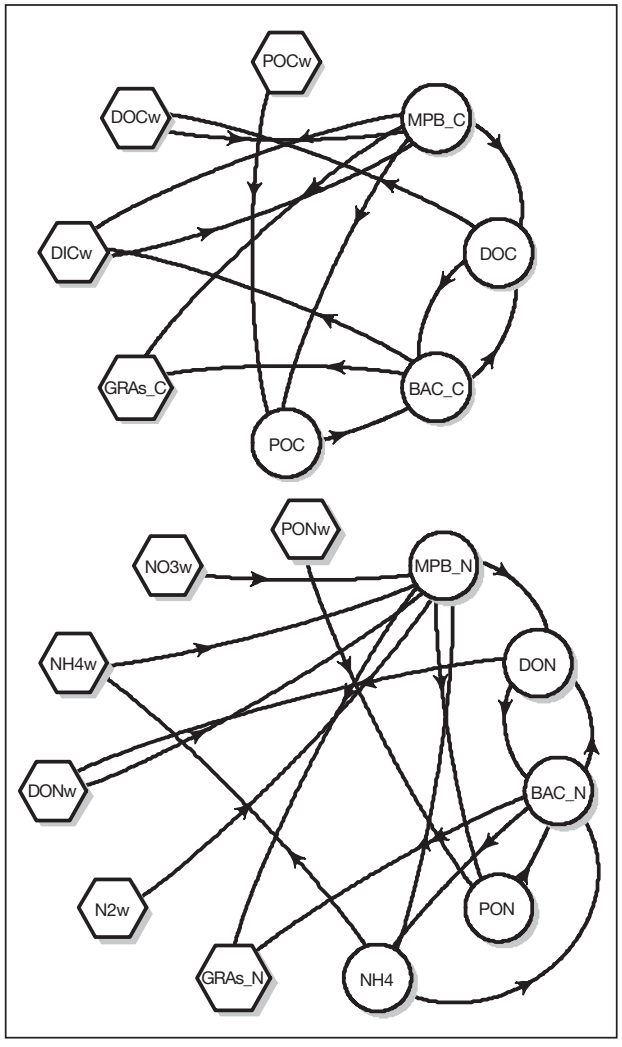

Fig. 2. Conceptual model used to reconstruct the carbon (_C) and nitrogen (_N) fluxes in the inverse analysis. w = species derived from the water column; BAC = bacteria; DIC = dissolved inorganic carbon; MPB = microphytobenthos; DOC, DON = dissolved organic carbon and nitrogen, respectively; POC, PON = particulate organic carbon and nitrogen, respectively; GRAs = Grazing; NH4 = ammonium (NH_4^+); NO3 = nitrate (NO_3^-); N2 = nitrogen (N_2)

The model structure described above is implemented in the linear inverse model as the matrix equation:

$$\mathbf{A}_{m\times n} \times \mathbf{x}_n = \mathbf{b}_m \quad (1)$$

where matrix **A** contains the m mass balances, one for each pool, vector **x** contains the n unknown fluxes in the model, and vector **b** contains the m time derivatives, one for each mass balance. For the sake of simplicity we will assume that the mass balances are in steady-state and hence the time derivatives in vector **b** are zero (in other words, the temporal variation of stocks was assumed to be insignificant compared to flows).

The current equation (Eq. 1) simply expresses the conceptual relationship between fluxes, but there are no quantitative constraints on the magnitudes of these fluxes. Such constraints are provided by measurements of nutrient fluxes across the sediment-water interface (e.g. NH_4^+ release/uptake and community respiration) and stoichiometric relations between C and N fluxes (Table 2). Each measurement can be written as a function of the fluxes in the model. For example, community respiration is the sum of the respiration fluxes by all the biotic compartments. As such, each measurement can be expressed as a linear function of the model fluxes and be appended as an additional row in the matrix equation Eq.1 (see Soetaert & Van Oevelen (2009) for a pedagogical example). Similarly, stoichiometric relations imply that some C and N flows are linked. For example, grazing of bacteria and MPB by fauna induces loss fluxes with a stoichiometric ratio that equals that of the respective source compartment. The stoichiometric relations implemented in the model are provided in Tables 3 & 4.

The matrix Eq. (1) is extended with the flux measurements and the stoichiometric relations (d) and becomes:

$$\mathbf{A}_{(m+d)\times n} \times \mathbf{x}_n = \mathbf{b}_{m+d} \quad (2)$$

in which matrix **A** contains the m mass balances and d flux measurements + stoichiometric relations, Vector **b** contains the m time derivatives (zero in this study)

Table 2. Mass balances of the biotic and abiotic pools in the inverse box model. Pool names are MPB = microphytobenthos; DIC = dissolved inorganic carbon; BAC = bacteria; POC, PON = particulate organic carbon and nitrogen, respectively; DOC, DON = dissolved organic carbon and nitrogen, respectively; NH4 = ammonium; GRAs = grazers. Suffixes: carbon (_C) and nitrogen (_N) = balance of the respective pool; w, s = sources considered from the water column and sediment, respectively. Mass balances relate the rate of change of each (here assumed to be 0) to sources minus sinks. $A \rightarrow B$ = flux from pool A to pool B

Pool	Mass balance
MPB_C	$dMPB\_C/dt = [DICw \rightarrow MPB\_C] + [DOCw \rightarrow MPB\_C] - [MPB\_C \rightarrow DICw] - [MPB\_C \rightarrow DOC] - [MPB\_C \rightarrow GRAsC] + [MPB\_C \rightarrow POC]$
MPB_N	$dMPB\_N/dt = [DONw \rightarrow MPB\_N] + [NH4 \rightarrow MPB\_N] + [NH4w \rightarrow MPB\_N] + [NO3w \rightarrow MPB\_N] + [N2w \rightarrow MPB\_N] - [MPB\_N \rightarrow DON] - [MPB\_N \rightarrow GRAs\_N] - [MPB\_N \rightarrow PON]$
BAC_C	$dBAC\_C/dt = [DOC \rightarrow BAC\_C] + [POC \rightarrow BAC\_C] - [BAC\_C \rightarrow DICw] - [BAC\_C \rightarrow DOC] - [BAC\_C \rightarrow GRAs\_C]$
BAC_N	$dBAC\_N/dt = [DON \rightarrow BAC\_N] + [PON \rightarrow BAC\_N] + [NH4 \rightarrow BAC\_N] - [BAC\_N \rightarrow NH4] - [BAC\_N \rightarrow DON] - [BAC\_N \rightarrow GRAs\_N]$
DOC	$dDOC/dt = [MPB\_C \rightarrow DOC] + [BAC\_C \rightarrow DOC] - [DOC \rightarrow BAC\_C] - [DOC \rightarrow DOCw]$
DON	$dDON/dt = [MPB\_N \rightarrow DON] + [BAC\_N \rightarrow DON] - [DON \rightarrow BAC\_N] - [DON \rightarrow DONw]$
POC	$dPOC/dt = [POCw \rightarrow POC] + [MPB\_C \rightarrow POC] - [POC \rightarrow BAC\_C]$
PON	$dPON/dt = [PONw \rightarrow PON] + [MPB\_N \rightarrow PON] - [PON \rightarrow BAC\_N]$
NH4	$dNH4/dt = [BAC\_N \rightarrow NH4] - [NH4 \rightarrow BAC\_N] - [NH4 \rightarrow MPB\_N] - [NH4 \rightarrow NH4wN]$

Table 3. Processes and stoichiometric relations implemented as equalities in the inverse model. EOM = extracellular organic material (further acronyms in Table 2)

Process expression in inverse model as a function of the fluxes	
Total sediment respiration =	[MPB_C → DICw] + [BAC_C → DICw]
Net NH_4^+ production =	[BAC_N → NH4] – [NH4 → BAC_N]
Net DON influx =	[DOCw → DOC] – [DON → DONw]
Benthic primary production (Primprod_C) =	DICw → MPB_C
Nitrogen fixation =	N2w → MPB_N
NH_4^+ assimilation MPB from sediment =	NH4 → MPB_N
NH_4^+ assimilation MPB from water column =	NH4w → MPB_N
NO_3^- assimilation MPB from water column =	NO3w → MPB_N
Total N assimilation (Primprod_N) =	[N2w → MPB_N] + [NH4 → MPB_N] + [NH4w → MPB_N] + [NO3w → MPB_N] + [DON → MPB_N]
EOM excretion =	Primprod_C – MPB_CN × Primprod_N
C:N coupling bacterial production	$[POC \rightarrow BAC\_C] + [DOC \rightarrow BAC\_C] - [BAC\_C \rightarrow DICw] = CN_{BAC} \times ([PON \rightarrow BAC\_N] + [DON \rightarrow BAC\_N] + [NH4 \rightarrow BAC\_N] - [BAC\_N \rightarrow NH4])$
C:N coupling bacterivory	[BAC_C → GRAs_C] = CNBAC × [BAC_N → GRAs_N]
C:N coupling herbivory	[MPB_C → GRAs_C] = CNMPB × [MPB_N → GRAs_N]

Table 4. Literature constraints imposed in the inverse model. See Table 2 for acronyms

Process and expression in inverse model		Min – Max	Source
Bacterial C growth efficiency = $\frac{[POC \rightarrow BAC\_C]+[DOC \rightarrow BAC\_C]-[BAC\_C \rightarrow DIC]}{[POC \rightarrow BAC\_C]+[DOC \rightarrow BAC\_C]}$		[0.15 – 0.40]	del Giorgio & Cole (1998)
Bacterial C turnover = $[POC \rightarrow BAC\_C]+[DOC \rightarrow BAC\_C]-[BAC\_C \rightarrow DIC]$		[0.016 × BAC_C – 1.6 × BAC_C]	Sander & Kalff (1993)
Grazed fraction of bacterial production = $\frac{[BAC\_C \rightarrow GRAs\_C]}{[POM\_C \rightarrow BAC\_C]+[DOM\_C \rightarrow BAC\_C]-[BAC\_C \rightarrow DIC\_C]}$		[0.0 – 0.30]	Van Oevelen et al. (2006b)
Gross ammonification =	$BAC\_N \rightarrow NH4$	Spring/summer [0.0 – 6.0]	Blackburn & Henriksen (1983)
		Autumn/winter [0.0 – 15.0] (mmol m^{-2} d^{-1})	Blackburn & Henriksen (1983)
MPB respiration =	$\frac{[MPB\_C \rightarrow DIC]}{[DIC \rightarrow MPB\_C]}$	[0.06 – 0.22]	Langdon (1993)
C:N ratio POM =	$\frac{[POC \rightarrow BAC\_C]}{[PON \rightarrow BAC\_N]}$	[7 – 17]	Assumed
C:N ratio DOM =	$\frac{[DOCw \rightarrow MPB\_C]}{[DONw \rightarrow MPB\_N]}$	[5 – ∞]	Burdige & Zheng (1998)

and *d* numerical flux data + numerical data related to the stoichiometric ratios.

Other quantitative information can be found in physiological considerations that impose relationships between fluxes. For example, the production of biomass costs energy, paid by respiration, and this can be taken into account by enforcing that a certain minimal fraction of C uptake must be respired. Quantitative information that enforces that fluxes (or a combination of fluxes) should be lower or larger than a certain value is included in a matrix equation with linear inequalities, which is given by:

$$\mathbf{G}_{c\times n} \times \mathbf{x}_n \geq \mathbf{h}_c \quad (3)$$

where matrix $\mathbf{h}_c$ contains the inequality coefficients, which signify how much a flux contributes to the inequality, and $\mathbf{G}_{c\times n}$ contains the values of the lower and upper bounds. Multiplying an upper boundary inequality with –1 transforms it in a lower boundary inequality, which can subsequently be implemented in Eq. (2). By default, all fluxes are subject to the inequality ≥0 to ensure that all fluxes have a direction. In case 2 opposing flows are present, the net flux can change direction depending on the magnitude of the opposing fluxes. Fluxes across the sediment-water interface can change direction, but for each data set, the direction was constrained by flux measurements (Table 1). In addition, we used the inequality equations to constrain the following: bacterial growth efficiency, respiration by MPB, bacterial C production, coupling of the uptake of dissolved organic carbon and nitrogen (DOC and DON, respectively) (since this can be uncoupled when only carbohydrates are taken up), the fraction of bacterial production that is grazed by fauna, coupling of bacterial uptake of C and N from sedimentary POC, and bacterial mineralization of NH_4^+ (Table 4). Again, we refer to Soetaert & Van Oevelen (2009) for a pedagogical example on the implementation of physiological constraints.

The number of equalities in the inverse model (9 mass balances and 12 data equalities) is lower than the number of fluxes (28) to be estimated, which makes the model mathematically under-determined. This underdeterminacy implies that, if the data are consistent, the inverse model has infinite different solutions that all solve the mass balances and data equalities and comply with the inequalities. In early linear inverse modelling applications, a final solution was selected from this infinitely large set by an optimization criterion (Vézina & Platt 1988). Such an optimization criterion is a practi-

cal solution and ensures standardization in the solution method of inverse models. However, this optimization criterion is based on a minimization of the sum of squared flows, and it is presently unknown whether the selected solution really resembles the 'true' solution (Kones et al. 2006). Moreover, most inverse studies have not given an account on the uncertainty that is associated with the inferred flux values, although sensitivity analysis on the input data generally show that the inferred fluxes are not very sensitive to changes in the input data of the model (Jackson & Eldridge 1992, Niquil et al. 1998, Vézina & Savenkoff 1999).

A novel method was suggested by Kones et al. (2006), which is based on sampling the infinite set of solutions. In brief, the data in the matrix Eqs. (1) & (2) define a solution space that contains all valid solutions to the inverse model. A Monte Carlo sampling method takes random jumps in this solution space by a mirror algorithm that uses the inequality constraints as reflection planes (Van den Meersche et al. 2009). With every jump, a new solution is sampled such that the solution space becomes uniformly sampled. After sampling a sufficient number of solutions (10 000 for the present model), the whole solution space is covered by the sampling. The mean of this set of sampled solutions is taken as an average model solution and the SD is taken as an uncertainty measure (see Soetaert & Van Oevelen 2009 for details), which has been found to represent a good measure of uncertainty (Kones et al. 2006). Flux estimates that are well defined by the data will have low standard deviations, whereas fluxes that are poorly defined will have a high SD (Van Oevelen et al. in press). All models were run in the GNU software package R (R Development Core Team 2008) using the packages limSolve and LIM (Soetaert & Van Oevelen 2008). Subsequent statistical analysis were also undertaken in R

RESULTS

We first note that for each data set (site and season), an identical set of measurements was available, with the exception of N_2 fixation which was measured in the subsequent year. N_2 fixation rates were generally insignificant except during summer at Site CF, when they were in the upper range of rates reported in the literature. The N_2 fixation rates at Site CF are, therefore, most likely an upper estimate, and the measurements at other times and sites, a lower estimate. All the model runs could be solved for MPB cellular C:N ratios of 8 (mol:mol, the default) and 5. At a C:N ratio of 15, all runs could be solved for Site CF, but only 2 models could be solved for Site PC (PC_loaut [lower mudflats in autumn] and PC_upspr [upper mudflats in spring]). The models of Site PC that could not be solved with a MPB C:N = 15 had a comparatively high primary production of N as compared to C production. The constraint on EOM production (Table 3) combined with a C:N ratio of 15 would imply a negative EOM release. Further runs of these models showed that the threshold for a solvable model was at a MPB C:N ratio of ~8 to 10. In general, the fluxes were well defined, with 50 and 90% of the flows having relative SDs <36 and 70%, respectively (Fig. 3). The highest relative uncertainties generally surrounded the release of EOM by MPB and the grazing on MPB (Tables S1–S3, available as Supplementary Material at: www.int-res.com/articles/suppl/m394p035_app.pdf).

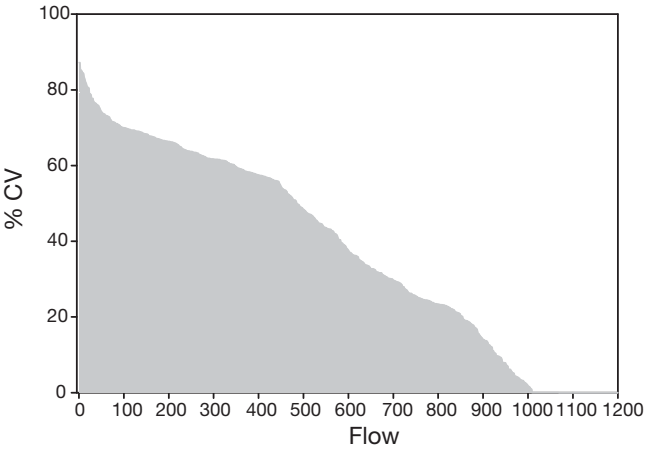

Fig. 3. The percentage CV (SD/mean × 100) for each of the ~1200 fluxes (i.e. fluxes in all 16 models using C:N of 8 for microphytobenthos) estimated in this study, derived from the set of sampled solutions for each model (see 'Inverse method')

The model runs for each data set reflected the higher productivity and generally more autotrophic nature of the mudflat at Site CF as compared to Site PC by the larger fluxes of C between the model compartments (Fig 4) as identified by (Cook et al. 2004a). Grazing of MPB was generally a minor flux for C, but was more important for N. POM from the water column was an important flux of C and N to the sediment equivalent to 14–550% of C fixation by MPB and 22–260% of N uptake by MPB. During summer, N_2 fixation dominated the form of N assimilated by MPB at Site CF_{upper}, consistent with abundant cyanobacteria observed at that site at the time (Cook et al. 2004c). Fluxes of DON frequently dominated over DIN fluxes and there were often large fluxes of DOC from the sediment to the water column. Furthermore, the model results suggest intense recycling of DON and DOC between the bacteria and the sediment pool during virtually all of the sampling events (Tables S1–S3).

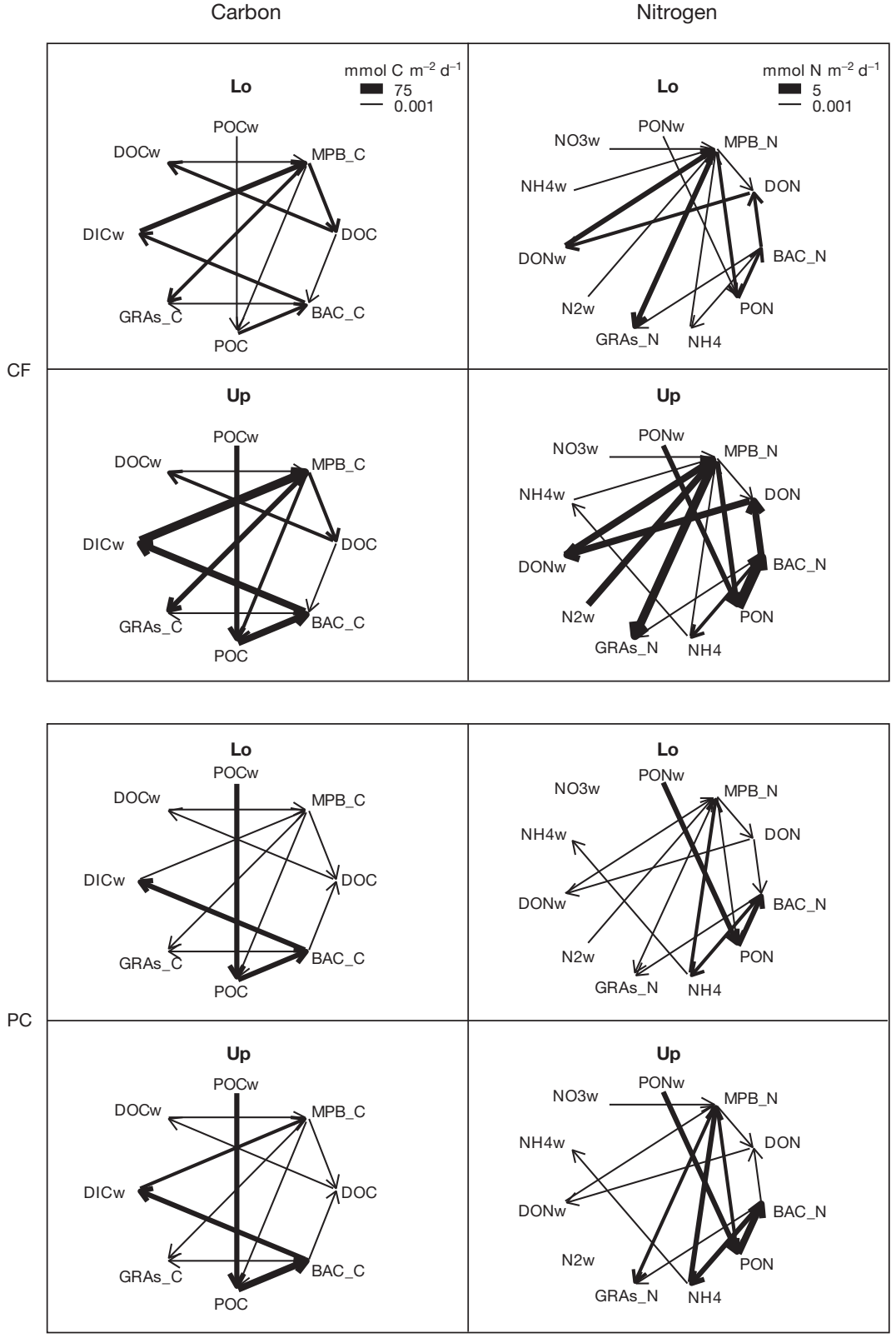

Fig. 4. Examples of fluxes of C and N through the microbial compartments on the upper (Up) and lower (Lo) mudflats of Castle Forbes Bay (CF) and Port Cygnet (PC) during summer. Fluxes are from model results with microphytobenthos C:N ratio = 8 (see 'Materials and methods' for further information). See Fig. 2 for acronyms

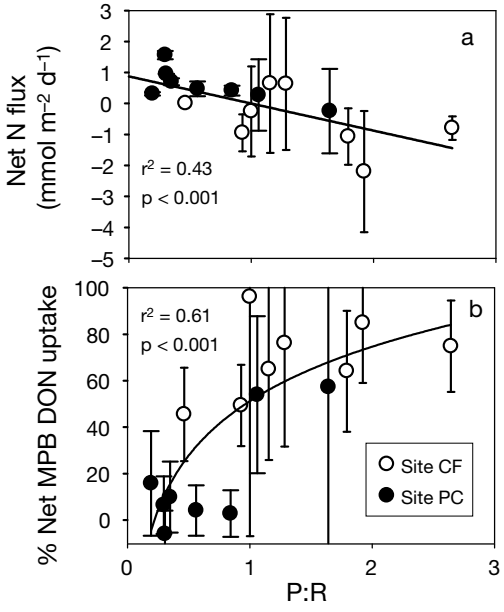

Fig. 5. (a) net N flux across the sediment-water interface, (b) percentage of N assimilated as dissolved organic N (DON) by microphytobenthos (MPB) as a function of P:*R*. CF: Castle Forbes Bay; PC: Port Cygnet. Error bars = SD of each process derived from the set of sampled solutions using Monte Carlo sampling (see 'Inverse method' section for details)

The sediments acted as either net sources or sinks for N, with net daily fluxes of all N containing compounds ranging between –2.2 mmol m^{-2} d^{-1} (uptake) during spring at Site CF_{upper}, and 1.5 mmol m^{-2} d^{-1} (release) at Site PC_{upper} during autumn. There was generally no release of inorganic N from the sediment under autotrophic conditions (particularly at Site CF) because of N uptake by MPB at the sediment water interface. Under heterotrophic conditions, fluxes of N across the sediment water interface were dominated by a release of NH_4^+. The net daily N flux had a significant negative relationship with P:*R* (r^2 = 0.43, p < 0.001) and the sediments were, on average, a net source of N to the water column at P:*R* < 1 and a net sink at P:*R* > 1 (Fig. 5a). The net assimilation of DON by MPB generally comprised >50% of total net N assimilated under autotrophic conditions, whilst under heterotrophic conditions (P:*R* < 1), net DON assimilation generally comprised <10% of total net N assimilation (Fig 5b). Between 0 and 64% of C fixation was excreted as EOM, with mean (±SD) being 39 ± 13% at Site CF and 18 ± 8% at Site PC when the cell C:N ratio was fixed to 8. Stepwise multiple regression analysis showed that the MPB cellular C:N ratio (as determined by the 3 model scenarios) contributed significantly (p < 0.05) to the percentage of EOM production, the DIC:N ratio assimilated by MPB, and the C:N ratio of EOM (Figs 6a–c). Increasing the MPB cellular C:N ratio decreased the percentage of C

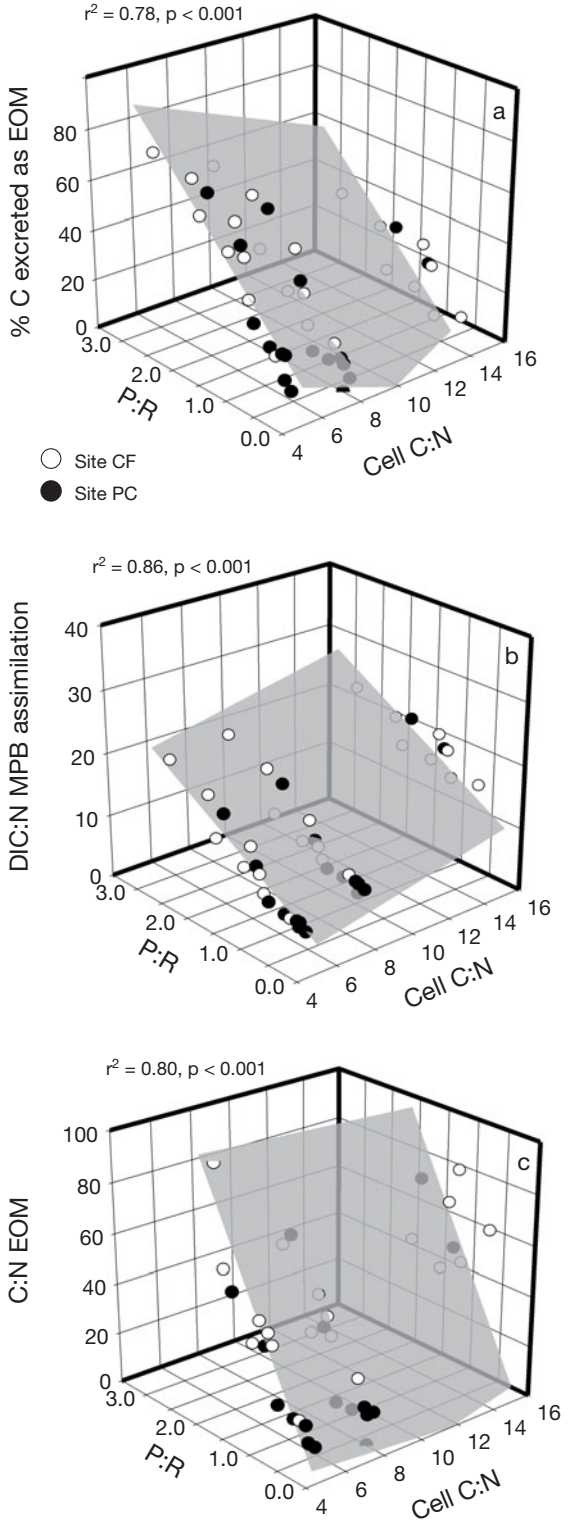

Fig. 6. (a) percentage of C fixed, excreted as extracellular organic material (EOM) by MPB, (b) DIC:N uptake ratio by MPB, and (c) C:N ratio of DOM excreted by MPB as a function of P:*R* and cell C:N ratio. CF: Castle Forbes Bay; PC: Port Cygnet. Multiple regression planes and equations are shown

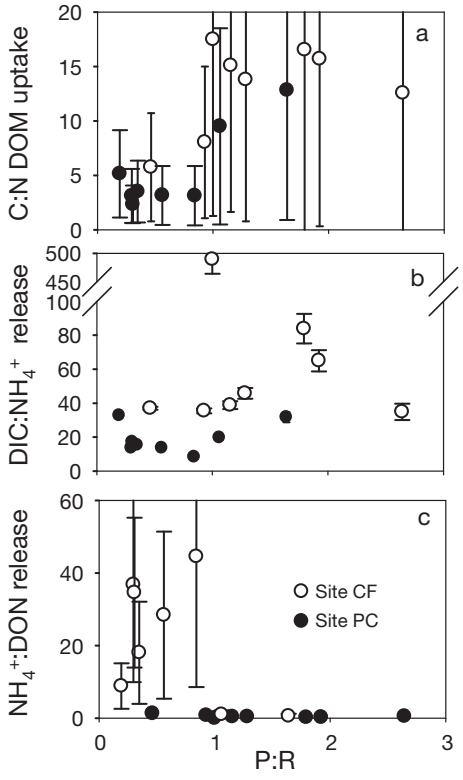

Fig. 7. (a) C:N of DOM taken up by bacteria, (b) DIC:NH_4^+ released by bacteria, and (c) NH_4^+:DON released by bacteria as a function of sediment P:*R*. CF: Castle Forbes Bay; PC: Port Cygnet. Error bars = SD of each process derived from the set of sampled solutions using Monte Carlo sampling (see 'Inverse method' section for details)

excreted as EOM, and increased the DIC:N assimilation ratio and the C:N of EOM released by MPB.

The C:N ratio of DOM taken up by bacteria increased abruptly from ~4 under heterotrophic conditions (P:*R* < 1) up to 15 under autotrophic conditions (P:*R* > 1, Fig. 7a). The net release of DIC:NH_4^+ by bacteria was high, particularly at Site CF where it was always >30, reaching up to 490 during autumn at Site CF_{lower}. At Site PC, by contrast, the ratio of DIC:NH_4^+ was generally <20 and averaged 19, only slightly above the average sediment C:N ratio of 15 at that site. The ratio of DIC:NH_4^+ production by bacteria had no significant relationship to P:*R*, although DIC:NH_4^+ production by bacteria was significantly higher under autotrophic conditions (t-test, $p < 0.05$, data log transformed, Fig 7b). Similarly, the ratio of NH_4^+:DON released by bacteria was significantly different under autotrophic and heterotrophic conditions (t-test, $p < 0.005$, Fig 7c). Under heterotrophic conditions, NH_4^+ release by bacteria dominated over DON (mean NH_4^+:DON = 22), whereas under autotrophic conditions, the release of DON dominated over NH_4^+ (mean NH_4^+:DON = 0.43).

DISCUSSION

The aim of this study was to reconstruct the C and N fluxes through the microbial community and the influence of sediment metabolism on these. The biogeochemical measurements previously made in this system are complicated by the fact that the observed fluxes are often the net outcome of a number of competing processes. For example, ammonia production within the sediment is the net balance between ammonia assimilation and release by bacteria. Furthermore, many processes, such as EOM production by MPB and subsequent assimilation by bacteria could not be measured to a high degree of accuracy in intact cores owing to methodological constraints. Finally, resource limitations meant that it was impossible to apply all available methods simultaneously to constrain all possible processes. The inverse analysis undertaken here allows us to reconstruct unmeasured flows within the mudflat sediments. We note that some of the processes have been measured (for example, the net flux of C and N across the sediment-water interface) and the inverse analysis adds no information to these measured fluxes as compared to a simple analysis of the raw data. In the following discussion we focus on the fluxes of C and N between MPB and bacteria, which were not directly measured and have been reconstructed using the inverse analysis. We note that this is the first time such a data set has been analysed in this way, and that this analysis allowed us to shed new light on the decoupling of C and N flows through algae and bacteria caused by EOM excretion across a range of P:*R* values.

The application of linear inverse modelling ensures that flux estimates are based on mass balances and are plausible in terms of parameters such as bacterial growth efficiency and turnover. Inverse models are however mostly under-determined because there are fewer measurements that unknown fluxes. The strategy in inverse modelling is actually to exclude solutions that are inconsistent with the field observations and literature data. All solutions in the remaining set are all equally likely from a data-perspective. A prominent problem is the subsequent selection of one solution from this set that is presented as 'best' solution. A popular selection criterion has been to apply a parsimony principle and select the solution that has the minimal sum of squared flux values (Vézina & Platt, 1988). There are, however, also downsides to this principle: since the parsimony principle is not based on ecological theory, flux values are typically positioned at the lower or upper boundaries and this solution typically recovers zeros for some of fluxes in the model (Steele 2009). The search for a selection criterion that is better rooted in ecological theory is still ongoing (Véz-

ina et al. 2004). An alternative method has been proposed: Kones et al. (2009) and Soetaert & Van Oevelen (2009) sampled a representative set of solutions from all valid solutions. The average and SD for each flow in the sampled set was chosen as 'best' estimate and associated uncertainty for each flux, respectively. Although this method is also not based on ecological theory, it draws the solution away from the boundaries and avoids zeroing out fluxes in the model (Kones et al. 2006). Moreover, a direct estimate is obtained on the uncertainty with which the flux can be recovered. Our method cannot guarantee that the results presented here are a true representation of reality; the fluxes are a mere best derivative based on available data. We therefore discuss the plausibility of the model results presented here with respect to that available in the literature. Furthermore, we synthesise the implications of this analysis into a broader understanding of the influence of MPB on sediment biogeochemical function.

The net trophic status of the sediment (P:*R*) exerted a strong control over the dynamics of both N and C. Fundamentally, this manifested itself as a transition from the sediments being a net source of N under heterotrophic conditions to a net sink under autotrophic conditions (Fig 5a) as has been previously observed in the literature (e.g. Ferguson et al. 2004b, Sundbäck et al. 2004, Engelsen et al. 2008). When the sediment compartment becomes autotrophic, there is a net demand for N that must be supplied from the water column. In oligotrophic and mesotrophic waters, such as those in the Huon Estuary, the N supply rate from the water column will be low. Therefore, MPB in autotrophic sediments in mesotrophic to oligotrophic waters is likely to become N limited. Evidence to support this comes from the clear increase in the DIC:N ratio assimilated by MPB as the sediment becomes increasingly autotrophic (Fig. 6b).

The effects of N limitation on MPB are twofold: Firstly, there will be an increase in the cellular C:N ratio above 'ideal' proportions (Hillebrand & Sommer 1999), and secondly, MPB will excrete C (often referred to as extracellular polymeric substances, or EPS) through 'overflow' metabolism (Staats et al. 2000, Underwood 2002). The model analysis showed that the estimated proportion of C fixed that is excreted as EOM also depends on the cellular C:N ratio (Fig 6a). Because the C:N ratio has not been measured at each site and season, the exact effect of sediment P:*R* on C excretion rates is also uncertain. Based on the field data we do have from the study sites, we have constrained the cellular C:N ratio in the range of 5 to 15, and ran each model with 3 ratio values (5, 8 and 15). Under net heterotrophic (and relatively N replete) conditions, the cellular C:N ratio will be closer to 5 and the proportion of C excreted will tend towards the lower range of ~20% of total C fixed. As the P:*R* ratio (and relative N limitation) increases, the cellular C:N ratio will increase towards 15 and, hence, the proportion of C excreted will tend toward the lower range of ~30% of total C fixed (Fig 6a). We therefore estimate that the C excretion rate by MPB ranges from ~20% under heterotrophic conditions to >30% of production under autotrophic conditions. The overall range of ~0 to 60% C excretion estimated by the model covers the range of ~2 to 70% reported in the literature (Underwood & Paterson 2003).

The model results suggest that the C:N ratio of the EOM produced is generally in the range of 10 to 60 (Fig 6c), consistent with previous studies, which have shown excreted EOM to consist predominantly of carbohydrates, with amino acids and proteins comprising ~5 to 10% of the EOM (Staats et al. 1999, Granum et al. 2002). The highest C:N ratios of excreted EOM were observed at times of high DIC:N assimilation (most autotrophic conditions), which is consistent with the experiments of Staats et al. (2000) who showed that carbohydrate production increases rapidly upon nutrient limitation. 'Sloppy feeding' by grazers or viral lysis of MPB cells may also contribute to the release of OM (Brussaard 2004, Moller 2007) and this may be the major mechanism of EOM production under nutrient replete conditions. The C:N ratio of EOM exuded by algae has been rarely directly measured, and the limited data available suggest that under nutrient replete conditions, the C:N ratio of EOM is quite variable (~5 to 14) (Biddanda & Benner 1997, Wetz & Wheeler 2003, Van den Meersche et al. 2004), but rapidly increases beyond 16 under nutrient limited conditions (Wetz & Wheeler 2003, Van den Meersche et al. 2004). Thus, these literature data support our observation that the EOM derived from MPB can be relatively N poor, particularly under the most nutrient limited conditions.

Coincident with the increase in the C:N ratio of EOM excreted by MPB, there was also an increase in the C:N ratio of DOM taken up by bacteria (Fig 7a), suggesting that bacteria directly assimilate EOM excreted by MPB. This is consistent with previous studies that have shown that algal derived EOM is a highly bioavailable substrate for bacteria (van Duyl et al. 1999, Middelburg et al. 2000, Goto et al. 2001, Cook et al. 2007, Evrard et al. 2008). The metabolism of high C:N ratio EOM taken up by bacteria resulted in a relatively high ratio of DIC:NH_4^+ produced, particularly under net autotrophic conditions when the ratio was in the range of 20 to 480 (Fig. 7b). This relatively low release of inorganic N by bacteria is consistent with experiments on marine bacteria that have shown no net N mineralisation for substrates with a C:N ratio >10 (Goldman et al. 1987). This also accords with a previ-

ous study showing that nitrifying bacteria become starved of NH_4^+ in highly autotrophic sediments as a consequence of NH_4^+ uptake by heterotrophic bacteria stimulated by abundant availability of EOM (Risgaard-Petersen 2003).

Furthermore, the model demonstrated that bacterial production of DON dominated over NH_4^+ under autotrophic conditions when the DON release was ~2× the NH_4^+ release rate (Fig 7c). This finding is consistent with other studies over the past decade, which have shown the dominance of DON production over DIN within euphotic sediments (Lomstein et al. 1998, Pedersen et al. 1999, Berman & Bronk 2003). The reduced availability of DIN causes MPB to increasingly rely on DON as its N source as the sediments become more autotrophic (Fig 5b). This finding also accords with recent literature, which documents the assimilation of DON by pelagic algae (Berman & Bronk 2003), and that benthic algae can play an important role in mediating benthic DON fluxes (Tyler et al. 2003, Ferguson et al. 2004a, Veuger & Middelburg 2007). As such, increased sediment autotrophy leads to an increase in the relative importance of DON production and uptake within the microbial community.

Somewhat paradoxically, our previous discussion suggests a flow of DOC from MPB to bacteria via EOM under autotrophic conditions, whereas it can be seen (Fig 4 and Tables S1–S3) that there is generally a net flow of DOC from the bacteria to the DOC pool. Our explanation for this is that bacteria consume DOC from MPB (as well as POC), followed by a release of DOC through cell lysis (Van Oevelen et al. 2006b) resulting in a net flux of DOC from bacteria to the DOC pool. This mechanism also explains why there was generally a net flux of DON from bacteria to MPB. The DOM released by bacteria always had a low C:N ratio of ~5 (the extra N being derived from the POM pool), which was then taken up by N limited MPB. Thus, the cycling of N and C between the bacteria and MPB under autotrophic conditions was through organic forms alternating between high C:N ratio DOM from the MPB to the bacteria (a C source), followed by low C:N ratio DOM from the bacteria to algae (an N source).

CONCLUSIONS

The inverse analysis technique applied here provided a comprehensive mass balanced quantification of the C and N fluxes through MPB and bacteria within a conceptual framework consistent with *in situ* data and the literature. The net metabolic status of the sediment (P:*R*) had a clear impact on the cycling of C and N within the sediment. Under highly autotrophic conditions in the mesotrophic estuary studied, the C and N fluxes through MPB become highly decoupled and are well above the Redfield ratio. Bacteria consuming this high C:N ratio but labile material have, hence, a relatively low release of remineralised DIC relative to NH_4^+. These results highlight the fact that conventional stoichiometric assumptions about the fluxes of C and N cannot be made in highly autotrophic sediments. The inverse analysis also highlights the fact that a large proportion of the C and N fluxes pass through the organic pools (e.g. internal DON and DOC recycling within the sediment). In particular, we found the model outcomes with respect to C excretion by MPB to be highly sensitive to the cellular C:N ratio of MPB, which is often a poorly constrained parameter in field studies, and future work should particularly seek to constrain this parameter.

Acknowledgements. We thank 3 anonymous reviewers for constructive feedback on this work. P.L.M.C. thanks Dr. E Butler (CSIRO Marine and Atmospheric Research) for his support and encouragement in the collection of this data.

LITERATURE CITED

Berman T, Bronk DA (2003) Dissolved organic nitrogen: a dynamic participant in aquatic ecosystems. Aquat Microb Ecol 31:279–305

Biddanda BA, Benner R (1997) Carbon, nitrogen and carbohydrate fluxes during the production of particulate and dissolved organic matter by marine phytoplankton. Limnol Oceanogr 42:506–518

Blackburn TH, Henriksen K (1983) Nitrogen cycling in different types of sediments from Danish waters. Limnol Oceanogr 28:477–493

Brussaard CPD (2004) Viral control of phytoplankton populations: a review. J Eukaryot Microbiol 51:125–138

Burdige DJ, Zheng S (1998) The biogeochemical cycling of dissolved organic nitrogen in estuarine sediments. Limnol Oceanogr 43:1796–1813

Butler ECV, Parslow JP, Volkman JK, Blackburn SI and others (2000) Huon Estuary Study — environmental research for integrated catchment management and aquaculture. Final report to the Fisheries Research and Development Corporation project number 96/284. Report No. FRDC proj no 96/284, CSIRO Division of Marine Research. Marine Laboratories Hobart www.cmar.csiro.au/research/huonestuary/report/index.html

Cook PLM, Butler ECV, Eyre BD (2004a) Carbon and nitrogen cycling on intertidal mudflats of a temperate Australian estuary. I. Benthic metabolism. Mar Ecol Prog Ser 280: 25–38

Cook PLM, Revill AT, Butler ECV, Eyre BD (2004b) Carbon and nitrogen cycling on intertidal mudflats of a temperate Australian estuary. II. Nitrogen cycling. Mar Ecol Prog Ser 280:39–54

Cook PLM, Revill AT, Clementson LA, Volkman JK (2004c) Carbon and nitrogen cycling on intertidal mudflats of a temperate Australian estuary. III. Sources of organic matter. Mar Ecol Prog Ser 280:55–72

Cook PLM, Veuger B, Böer S, Middelburg JJ (2007) Effect of nutrient availability on carbon and nitrogen incorporation

and flows through benthic algae and bacteria in near shore sandy sediment. Aquat Microb Ecol 49:165–180

del Giorgio PA, Cole JJ (1998) Bacterial growth efficiency in natural aquatic systems. Annu Rev Ecol Syst 29:503–541

Engelsen A, Hulth S, Pihl L, Sundbäck K (2008) Benthic trophic status and nutrient fluxes in shallow-water sediments. Estuar Coast Shelf Sci 78:783–795

Evrard V, Cook PLM, Veuger B, Huettel M, Middelburg JJ (2008) Tracing incorporation and pathways of carbon and nitrogen in microbial communities of photic subtidal sands. Aquat Microb Ecol 53:257–269

Eyre BD, Ferguson AJP (2005) Benthic metabolism and nitrogen cycling in a subtropical east Australian estuary (Brunswick): temporal variability and controlling factors. Limnol Oceanogr 50:81–96

Ferguson A, Eyre B, Gay J (2004a) Nutrient cycling in the sub-tropical Brunswick estuary, Australia. Estuaries 27: 1–17

Ferguson AJP, Eyre BD, Gay JM (2004b) Benthic nutrient fluxes in euphotic sediments along shallow sub-tropical estuaries, northern New South Wales, Australia. Aquat Microb Ecol 37:219–235

Goldman JC, Dennett MR (2000) Growth of marine bacteria in batch and continuous culture under carbon and nitrogen limitation. Limnol Oceanogr 45:789–800

Goldman JC, Caron DA, Dennett MR (1987) Regulation of gross growth efficiency and ammonium regeneration in bacteria by substrate C:N Ratio. Limnol Oceanogr 32: 1239–1252

Goto N, Mitamura O, Terai H (2001) Biodegradation of photosynthetically produced extracellular organic carbon from intertidal benthic algae. J Exp Mar Biol Ecol 257: 73–86

Granum E, Kirkvold S, Mykelstad SM (2002) Cellular and extracellular production of carbohydrates and amino acids by the marine diatom *Skeletonema costatum*: diel variations and effects of N depletion. Mar Ecol Prog Ser 242: 83–94

Gribsholt B, Veuger B, Tramper A, Middelburg JJ, Boschker HTS (2009) Long-term ^{15}N-nitrogen retention in tidal freshwater marsh sediment: elucidating the microbial contribution. Limnol Oceanogr 54:13–22

Hillebrand H, Sommer U (1999) The nutrient stoichiometry of benthic microalgal growth: Redfield proportions are optimal. Limnol Oceanogr 44:440–446

Jackson GA, Eldridge PM (1992) Food web analysis of a planktonic system off Southern California. Prog Oceanogr 30:223–251

Joye SB, De Beer D, Cook PLM (2009) Biogeochemical dynamics of coastal tidal flats. In: Perillo GME, Wolanski E, Cahoon DR, Brinson MM (eds) Coastal wetlands: an ecosystem integrated approach. Elsevier, p 345–374

Kang CK, Kim JB, Lee KS, Kim JB, Lee PY, Hong JS (2003) Trophic importance of benthic microalgae to macrozoobenthos in coastal bay systems in Korea: dual stable C and N isotope analyses. Mar Ecol Prog Ser 259:79–92

Kones JK, Soetaert K, van Oevelen D, Owino JO, Mavuti K (2006) Gaining insight into food webs reconstructed by the inverse method. J Mar Syst 60:153–166

Kones JK, Soetaert K, van Oevelen D, Owino JO (2009) Are network indices robust indicators of food web functioning? A Monte Carlo approach. Ecol Model 220:370–382

Langdon C (1993) The significance of respiration in production measurements based on oxygen. ICES Mar Sci Symp 197:69–78

Lomstein BA, Jensen AGU, Hansen JW, Andreasen JB, Hansen LS, Berntsen J, Kunzendorf H (1998) Budgets of sediment nitrogen and carbon cycling in the shallow water of Knebel Vig, Denmark. Aquat Microb Ecol 14:69–80

Middelburg JJ, Barranguet C, Boschker HTS, Herman PMJ, Moens T, Heip CHR (2000) The fate of intertidal microphytobenthos carbon: an in situ ^{13}C-labeling study. Limnol Oceanogr 45:1224–1234

Moller EF (2007) Production of dissolved organic carbon by sloppy feeding in the copepods *Acartia tonsa*, Centropages typicus, and Temora longicornis. Limnol Oceanogr 52:79–84

Niquil N, Jackson GA, Legendre L, Delesalle B (1998) Inverse model analysis of the planktonic food web of Takapoto Atoll (French Polynesia). Mar Ecol Prog Ser 165:17–29

Pedersen AGU, Bernsten J, Lomstein BA (1999) The effect of eelgrass decomposition on sediment carbon and nitrogen cycling: a controlled laboratory experiment. Limnol Oceanogr 44:1978–1992

Pinckney JL, Carman KR, Lumsden SE, Hymel SN (2003) Microalgal-meiofaunal trophic relationships in muddy intertidal estuarine sediments. Aquat Microb Ecol 31: 99–108

R Development Core Team (2008) R: a language and environment for statistical computing. R Foundation for Statistical Computing, Vienna, Austria

Risgaard-Petersen N (2003) Coupled nitrification-denitrification in autotrophic and heterotrophic sediments: on the influence of benthic microalgae. Limnol Oceanogr 48: 93–105

Risgaard-Petersen N, Nicolaisen MH, Revsbech NP, Lomstein BA (2004) Competition between ammonia-oxidizing bacteria and benthic microalgae. Appl Environ Microbiol 70:5528–5537

Rizzo WM, Dailey SK, Lackey GJ, Christian RR, Berry BE, Wetzel RL (1996) A metabolism-based trophic index for comparing the ecological values of shallow-water sediment habitats. Estuaries 19:247–256

Sander BC, Kalff J (1993) Factors controlling bacterial production in marine and fresh-water sediments. Microb Ecol 26:79–99

Soetaert K, Van Oevelen D (2008) LIM: linear inverse model examples and solution methods. R package version 1.2

Soetaert K, Van Oevelen D (2009) Modeling food web interactions in benthic deep-sea ecosystems: a practical guide. Oceanography (Wash DC) 22:130–145

Staats N, de Winder B, Stal L, Mur LR (1999) Isolation and characterization of extracellular polysaccharides from epipelic diatoms *Cylindrotheca closterium* and *Navicula salinarum.* Eur J Phycol 34:161–169

Staats N, Stal LJ, Mur LR (2000) Exopolysaccharide production by the epipelic diatom *Cylindrotheca closterium*: effects of nutrient conditions. J Exp Mar Biol Ecol 249: 13–27

Steele JH (2009) Assessment of some linear food web methods. J Mar Syst 76:186–194

Sterner RW, Elser JJ (2002) Ecological stoichiometry: the biology of elements from molecules to the biosphere, Princeton University Press, Princeton, NJ

Sundbäck K, Enoksson V, Granéli W, Pettersson K (1991) Influence of sublittoral microphytobenthos on the oxygen and nutrient flux between sediment and water: a laboratory continuous flow study. Mar Ecol Prog Ser 74: 263–279

Sundbäck K, Linares F, Larson F, Wulff A, Engelsen A (2004) Benthic nitrogen fluxes along a depth gradient in a microtidal fjord: the role of denitrification and microphytobenthos. Limnol Oceanogr 49:1095–1107

Tyler AC, McGlathery KJ, Anderson IC (2003) Benthic algae

control sediment-water column fluxes of organic and inorganic nitrogen compounds in a temperate lagoon. Limnol Oceanogr 48:2125–2137

Underwood GJC (2002) Adaptations of tropical marine microphytobenthic assemblages along a gradient of light and nutrient availability in Suva Lagoon, Fiji. Eur J Phycol 37: 449–462

Underwood GJC, Paterson DM (2003) The importance of extracellular carbohydrate production by marine epipelic diatoms. In: Callow JA (ed) Advances in Botanical Research, Vol 40. Academic Press, London, p 183–240

Van den Meersche K, Middelburg JJ, Soetaert K, Rijswijk P, Boschker HTS, Heip CHR (2004) Carbon-nitrogen coupling and algal-bacterial interactions during an experimental bloom: modelling a ^{13}C tracer experiment. Limnol Oceanogr 49:862–878

Van den Meersche K, Soetaert K, Van Oevelen D (2009) xsample: an R function for sampling over- and underdetermined linear inverse problems. J Stat Softw 30:1–15

van Duyl FC, de Winder B, Kop AJ, Wollenzien U (1999) Tidal coupling between carbohydrate concentrations and bacterial activities in diatom-inhabited intertidal mudflats. Mar Ecol Prog Ser 191:19–32

Van Oevelen D, Soetaert K, Middelburg JJ, Herman PMJ and others (2006a) Carbon flows through a benthic food web: integrating biomass, isotope and tracer data. J Mar Res 64: 453–482

Van Oevelen J, Middelburg JJ, Soetaert KER, Moodley L (2006b) The fate of bacterial carbon in sediments: modelling an *in situ* isotope tracer experiment. Limnol Oceanogr 51:1302–1314

Van Oevelen D, Van den Meersche K, Meysman FJR, Soetaert K, Middelburg JJ, Vézina AF (in press) Quantitative reconstruction of food webs using linear inverse models. Ecosystems

Veuger B, Middelburg JJ (2007) Incorporation of nitrogen from amino acids and urea by benthic microbes: role of bacteria versus algae and coupled incorporation of carbon. Aquat Microb Ecol 48:35–46

Veuger B, Eyre BD, Maher D, Middelburg JJ (2007) Nitrogen incorporation and retention by bacteria algae and fauna in a sub-tropical intertidal sediment: an in-situ ^{15}N labelling study. Limnol Oceanogr 52:1930–1942

Vézina AF, Platt T (1988) Food web dynamics in the ocean. I. Best-estimates of flow networks using inverse methods. Mar Ecol Prog Ser 42:269–287

Vézina AF, Savenkoff C (1999) Inverse modeling of carbon and nitrogen flow in the pelagic food web of the northeast subarctic Pacific. Deep-Sea Res II 46:2909–2939

Vézina AF, Berreville F, Loza S (2004) Inverse reconstructions of ecosystem flows in investigating regime shifts: impact of the choice of objective function. Prog Oceanogr 60: 321–341

Wetz MS, Wheeler PA (2003) Production and partitioning of organic matter during simulated phytoplankton blooms. Limnol Oceanogr 48:1808–1817

Editorial responsibility: Alain Vézina, Dartmouth, Canada

Submitted: December 23, 2008; Accepted: August 14, 2009
Proofs received from author(s): November 11, 2009